A Generalized Approach for Predicting Coverage-Dependent Reaction Parameters of Complex Surface Reactions: Application to H_2 Oxidation over Platinum

Young K. Park, Preeti Aghalayam, and Dionisios G. Vlachos*

Department of Chemical Engineering, University of Massachusetts Amherst, Amherst, Massachusetts 01003

Received: May 19, 1999; In Final Form: August 16, 1999

A new methodology is presented for calculating parameters of complex surface reaction mechanisms. This approach takes into consideration adsorbate−adsorbate interactions along with their influence on the activation energies of surface reactions as a function of operating conditions. It combines an extension of the unity bond index−quadratic exponential potential theory, reactor scale modeling, important feature identification, and model validation. The H_2 oxidation over platinum has been chosen as a model system to test this methodology. Comparison with a variety of available experimental data in the literature, such as catalytic ignition temperature, laser-induced fluorescence OH desorption measurements, catalytic autotherms, and species profiles, shows that the proposed surface mechanism is capable of quantitatively capturing all the important features of the published experiments. Our approach offers the potential of quantitative modeling of catalytic reactors exhibiting complex surface reaction processes under realistic operating conditions.

Introduction

With the rapid advance in available computational power over the past decade, the ability to simulate reactors with a high level of complexity has become feasible. One example of a maturing field utilizing sophisticated modeling is catalytic combustion. It turns out that one of the major challenges in developing predictive models for catalytic combustion is the construction of reliable reaction mechanisms. While the homogeneous chemistry of various light fuels such as hydrogen and methane[14,22,11] is relatively well-known, large uncertainties exist in the parameters and even the reaction paths of surface reaction mechanisms.

The oxidation of H_2 over platinum is one of the most extensively studied systems and will be the focus of this paper. An array of different experimental techniques and data, such as laser-induced fluorescence (LIF),[12,42,20,13] temperature-programmed reaction (TPR),[10] molecular beam relaxation spectroscopy (MBRS),[1,39] second harmonic generation (SHG),[8] catalytic ignition temperatures,[31,6] and catalytic autotherms[9] have been employed. Despite the accumulated knowledge about this system, several issues still remain unclear. For example, for the key reaction OH* + H* → H_2O* (where * denotes an adsorbed species) on platinum, Ljungström et al. reports an activation energy of 0 kcal/mol,[20] Fridell et al. of 5.8 kcal/mol,[12] Williams et al. of 15 kcal/mol,[42] and Anton and Cadogan of 16 kcal/mol.[1] This apparent discrepancy in activation energies for the same reaction can be attributed in part to different experimental conditions, such as temperature, pressure, and fuel-to-oxidant ratio. Currently, none of the published mechanisms addresses this point.

Most surface science experiments are conducted under low or well characterized adsorbate coverages on single crystals and the role of adsorbate coverage in surface reaction pathways is known only for limited conditions. As a result, extrapolating reaction paths and parameters to conditions of practical interest (higher temperatures, pressures, and polycrystalline surfaces with different adsorbate coverages) poses a major difficulty. Currently, there is no systematic method to account for the effect of adsorbate−adsorbate interactions on reaction pathways that is appropriate for continuum reactor scales. While the major reaction pathways of H_2 oxidation over platinum have been studied, for more chemically complex fuels of practical interest such as methane (and higher alkanes), many of the reactions steps are poorly understood. In the latter case, the major difficulty is kinetic parameter estimation for many reactions without any guidance from reliable experimental data. Successful modeling of catalytic oxidation reactors demands a fundamental understanding of the aforementioned issues.

Here, we apply the foundations of the unity bond index−quadratic exponential potential (UBI-QEP) or bond order conservation (BOC) theory of Shustorovich, Bell, Sellers, and co-workers[35] to develop a quantitative surface reaction mechanism for the H_2 oxidation on polycrystalline platinum. We have extended the UBI-QEP theory to account for the effect of surface coverage on the energetics of surface reactions by incorporating adsorbate heats of chemisorption as a continuous function of surface coverage (see also below). The resulting surface reaction mechanism is coupled to reactor scale models and refined and validated against a wide range of experimental data, such as catalytic ignition, catalytic autotherms, reactant conversion, and LIF OH measurements, through a computational approach discussed next.

Computational Approach

The detailed reaction mechanism for the oxidation of H_2 is outlined in Table 1. The reaction mechanism assumes that gaseous H_2 and O_2 chemisorb dissociatively on the platinum surface producing H* and O*. The oxidation of H* begins with the addition of O* to form OH*. Subsequently, H_2O* can form either by the reaction H* + OH* → H_2O* or 2OH* → H_2O* + O*. Desorption steps of H_2O* and the intermediates H*, O*, and OH* are also considered. In all, there are nine reversible surface reactions. An Arrhenius type dependence is assumed

* To whom correspondence should be addressed. E-mail: vlachos@ecs.umass.edu.

10.1021/jp9916485 CCC: $18.00
Published on Web 09/16/1999

TABLE 1: Catalytic H_2 Oxidation Mechanism on Platinum[a]

	reaction	pre-exponential (s^{-1}) or sticking coeffiecient	activation energy (kcal/mol) $\theta^* = 1$	$\theta_H = 1$	$\theta_O = 1$
(1f)	$H_2 + 2^* \rightarrow 2H^*$	0.50	0.0	0.0	0.0
(1b)	$2H^* \rightarrow H_2 + 2^*$	1.0×10^{12}	20.0	14.0	20.0
(2f)	$O_2 + 2^* \rightarrow 2O^*$	0.03	0.0	0.0	0.0
(2b)	$2O^* \rightarrow O_2 + 2^*$	1.0×10^{13}	51.0	51.0	19.0
(3f)	$H^* + O^* \rightarrow OH^* + *$	1.0×10^{11}	12.1	8.8	13.4
(3b)	$OH^* + * \rightarrow H^* + O^*$	1.0×10^{11}	24.4	25.9	18.4
(4f)	$H^* + OH^* \rightarrow H_2O^* + *$	1.0×10^{10}	12.4	9.3	0.0
(4b)	$H_2O^* + * \rightarrow H^* + OH^*$	1.0×10^{11}	18.4	20.2	39.1
(5f)	$2OH^* \rightarrow H_2O^* + O^*$	1.0×10^{11}	18.9	18.9	0.0
(5b)	$H_2O^* + O^* \rightarrow 2OH^*$	1.0×10^{11}	12.6	12.6	34.1
(6f)	$OH + * \rightarrow OH^*$	1.00	0.0	0.0	0.0
(6b)	$OH^* \rightarrow OH + *$	5.0×10^{14}	63.0	63.0	30.0
(7f)	$H_2O + * \rightarrow H_2O^*$	0.70	0.0	0.0	0.0
(7b)	$H_2O^* \rightarrow H_2O + *$	1.0×10^{13}	10.0	10.0	10.0
(8f)	$H + * \rightarrow H^*$	1.00	0.0	0.0	0.0
(8b)	$H^* \rightarrow H + *$	1.0×10^{13}	60.2	55.4	60.2
(9f)	$O + * \rightarrow O^*$	1.00	0.0	0.0	0.0
(9f)	$O^* \rightarrow O + *$	1.0×10^{13}	92.6	92.6	67.0

[a] For each reaction, the reaction pre-exponential as well as the model-computed activation energies are shown. For the activation energies, three limiting cases of the surface coverages are shown, a clean surface ($\theta^* = 1$), an H* covered surface ($\theta_H = 1$), and an O* covered surface ($\theta_O = 1$). Only pre-exponentials which differ from 10^{11} s^{-1} and 10^{13} s^{-1} have been optimized.

for all reaction rate constants

$$k = A \exp(-E_a/RT) \tag{1}$$

where A is the preexponential, E_a is the activation energy, R is the ideal gas constant, and T is the temperature.

Since our goal is to construct a surface reaction mechanism for predictive modeling at typical reactor conditions, we have chosen polycrystalline platinum as our catalyst. However, when the desired experimental information for polycrystalline platinum is not available in the literature, we have used data available for Pt(111) as discussed below.

Our overall approach starts with estimations of the heats of chemisorption of surface species. We subsequently use the UBI-QEP framework to compute the energetics of surface reactions on the fly of a continuation simulation, i.e., as a parameter (e.g., surface temperature or composition) is systematically varied using initially assigned pre-exponentials. Finally, the initially assigned pre-exponentials are refined through model identification techniques discussed below. This procedure is outlined next.

Coverage-Dependent Adsorption−Desorption Parameters. We first summarize experimental information on adsorption−desorption steps, which will subsequently be used to determine heats of chemisorption and energetics of surface reactions.

Adsorption−Desorption of Hydrogen. The available experimental data on Pt(111) indicate that the adsorption process is nonactivated[5] with the sticking probability decreasing linearly with increasing H* coverage.[43] The chemisorption of H_2 is therefore expressed as

$$S(H_2) = S^\circ(H_2)\theta^* \tag{2}$$

with S the coverage-dependent sticking coefficient, S° the sticking coefficient on a clean surface, and θ^* the fraction of the vacant surface sites. The actual value of $S^\circ(H_2)$ depends strongly on the type of platinum surface. For example, Somorjai reports $S^\circ(H_2) \leq 0.001$ for defect-free Pt(111), 0.01 for Pt(111), and ~0.9 for stepped Pt(332).[36] Higher values of $S^\circ(H_2)$ are therefore attributed to the surface roughness, steps, and defects of the platinum surface. Since some surface roughness and inhomogeneities are expected for a working catalyst, we have chosen an intermediate $S^\circ(H_2)$ value of 0.5 for the model.

For the associative desorption of H*, there are some differences in the reported experimental data. On one hand, Christmann et al.[5] report an activation energy of desorption of ~9.5 kcal/mol from a clean Pt(111) surface through temperature-programmed desorption (TPD) experiments. They have also observed two desorption peaks and interpreted their data by a lateral H*−H* repulsive energy of ~2 kcal/mol. Norton et al.,[24] on the other hand, have used deuterium nuclear microanalysis and reported an activation energy of desorption on a clean Pt(111) surface of ~16 kcal/mol, with a repulsive H*−H* interaction energy of ~8 kcal/mol at 0.7 monolayer. Researchers have attributed these differences to the structural differences of the platinum surface, with an increase in the binding energy of H* with increasing structural imperfections.[5] Values as high as 25 kcal/mol for the activation energy of desorption of H* from a platinum wire have been reported.[25] Taking the above information into consideration, we have defined the activation energy of desorption of H* as

$$E_a\,(\text{kcal/mol}) = 20.0 - 6.0\theta_{H^*} \tag{3}$$

We should remark here about thermodynamic consistency of surface reaction mechanisms. In the past, while researchers have used such a functional dependence of the activation energy of desorption on surface coverage, these expressions were not necessarily used in reactor models in a thermodynamically consistent manner. Since the details of the kinetics may not always be included in a reaction mechanism (e.g., multiple different paths for adsorption such as molecular, dissociative, percursor mediated, etc.), we have used experimental data about the adsorption/desorption steps instead of using the UBI-QEP formalism. As a result, the difference in the activation energies of the adsorption/desorption steps (eqs 2−5) may not exactly reflect the heats of reactions which should be the case for elementary reactions. Therefore, to ensure that our computed heats of reactions are thermodynamically consistent, the heats of all surface reactions are referenced against their analogous gas-phase reaction.

Adsorption−Desorption of Oxygen. The parameters of the dissociative adsorption and associative desorption of O_2 have also been inferred from experimental data available in the literature, which indicate that the adsorption is nonactivated (at least for low coverages, ≤0.25) with the sticking coefficient decreasing quadratically with increasing O* coverage.[21,43] The chemisorption of O_2 can therefore be expressed as

$$S(O_2) = S^\circ(O_2)\theta^{*2} \tag{4}$$

Several values for the sticking coefficient of O_2 on a clean Pt(111) surface, $S^\circ(O_2)$, have been reported in the literature, ranging from ~0.02[36] to ~0.05.[4] On the basis of these experimental findings, we have chosen an intermediate value of 0.03.

For the desorption, the activation energy on Pt(111) is found to be ~51 kcal/mol on a clean platinum surface, decreasing by ~8 kcal/mol for 0.25 monolayer O* coverage.[4] We recognize that in many surface science experiments the saturation O* coverage attained with O_2 has been 0.25. However, these experiments have typically been conducted at low pressures, which are unlikely for realistic process. A study of high O* coverage on Pt(111) using NO_2 instead of O_2 indicates that coverages of up to θ_O ~0.8 can be achieved.[28] TPD shows that while the interaction between O*−O* can be complex, there is

a net repulsive interaction of ~32 kcal/mol at high θ_O.[28] We have therefore taken a simple linear relationship for the repulsive O*−O* interactions, with the activation energy of desorption expressed as

$$E_a\,(\text{kcal/mol}) = 51.0 - 32.0\theta_{O^*} \qquad (5)$$

Adsorption−Desorption of Hydroxyl. The molecular adsorption of OH is assumed to be nonactivated with an initial sticking coefficient of 1.0 which depends linearly on the fraction of empty sites. The desorption of OH* has been studied in detail through LIF experiments. The results indicate that the apparent activation energy of desorption depends strongly on the H_2/O_2 ratio. For polycrystalline platinum, the apparent activation energy ranges from as high as ~60 kcal/mol at high H_2/O_2 ratios to as low as ~30 kcal/mol at low H_2/O_2 ratios.[13,23,41] It has been speculated that, at high H_2/O_2 ratios, adsorbate coverages on the platinum surface are very low[12] and the apparent activation energy of ~60 kcal/mol represents the binding energy of OH* on a clean platinum surface. As the H_2/O_2 ratio decreases, the surface coverage of O* increases and the limit of ~30 kcal/mol represents the binding energy of OH* in the presence of O*. This lowering of the binding energy of OH* in the presence of O* is speculated to be a net result of an attractive interaction due to hydrogen bonding of OH* to O* and a repulsive interaction between the O atom in OH* and O*.[26] We have therefore taken the activation energy of OH* to depend on O* coverage according to

$$E_a\,(\text{kcal/mol}) = 63.0 - 33.0\theta_{O^*} \qquad (6)$$

Adsorption−Desorption of Water. For the adsorption of H_2O, based on Pt(111) data, we have assumed the sticking coefficient of 0.7 and a zero activation energy, while for the desorption, we have taken the literature reported desorption activation energy of ~10 kcal/mol and pre-exponential of 10^{13} s^{-1}.[37]

Adsorption−Desorption of Radicals H and O. We have also included the adsorption and the desorption steps of radicals H and O. While not considered important at low catalyst temperatures, very small concentrations of H and O radicals are known to be important in promoting or triggering the homogeneous ignition of H_2.[17] Desorption of H* and O* could be important at high-temperature reactor operation, such as during catalyst-assisted homogeneous combustion.[29] However, since limited information is available from the literature for these steps, we have assumed the adsorption to be nonactivated with a sticking coefficient of 1.0 and expressed the desorption activation energy as the heat of chemisorption.

Coverage-Dependent Energetics and Pre-exponentials of Surface Reactions. For the rest of the surface reactions, the activation energies are computed using the UBI-QEP theory of Shustorovich. The details of the theory as well as its application are available in the literature.[35,34] Briefly, UBI-QEP describes the energetics of the interaction of an adsorbate and a transition metal atom with a potential that depends quadratically on the bond order. In this case, a Morse potential is used. Only nearest neighbor interactions between an adsorbate and the transition metal atoms are considered, with the total energy of the system represented as the sum of pairwise additive Morse interactions. Energetics of surface reactions are computed through a constrained optimization of the energy along the reaction coordinate, represented in terms of the bond order of the system.[33] The resulting activation energies of the surface reactions can conveniently be expressed only in terms of the heats of chemisorption and the gas-phase enthalpy of formation of the species involved in the reaction. In other words, within the context of the UBI-QEP theory, the specific details of the adsorbate-to-metal interactions are represented by the heat of chemisorption, which is an experimentally measurable quantity. The concept of the heat of chemisorption influencing the surface reaction activation energies was originally suggested by Shustorovich[32] and demonstrated for specific examples of adsorbate coverages. Here, by expressing the heats of chemisorption of surface species as a continuous function of surface coverage, we have extended the UBI-QEP theory to directly calculate the reaction activation energies under different reactor conditions, i.e., take into account the effect of adsorbate−adsorbate interactions on energetics.

As described previously, only three types of adsorbate−adsorbate interactions are taken into consideration in this reaction mechanism: H* to H*, O* to O*, and OH* to O* interactions. While other adsorbate−adsorbate interactions may exist, there is limited available reliable experimental data in the literature. However, our approach and code can consider complete multicomponent adsorbate interactions and a functional form of interactions that is different from linear.

The gas-phase enthalpies of all species involved in the H_2 oxidation mechanism are readily available in the literature (here, we use the CHEMKIN thermodynamic database[19]), so only the heats of chemisorption of these species are needed to compute surface reaction energetics. The heats of chemisorption have been computed using experimental data described by eqs 3, 5, and 6 and the UBI-QEP framework.

Since UBI-QEP theory provides only the energetics of reactions, another important factor is estimation of the reaction pre-exponentials. For chemisorption, the approximate (initial) values of sticking coefficients have been taken from literature reported values, as discussed above. For all other pre-exponentials, we have initially assumed a value of 10^{11} s^{-1} for surface reactions and 10^{13} s^{-1} for desorption (typical values from transition state theory) and refined them through comparison with various experimental data as discussed below.

Reactor Models, Feature Identification, and Parameter Refinement. At high pressures, the resulting surface reaction mechanism is coupled with the stagnation flow model of Bui et al.[2] Briefly, this continuum model converts the coupled two-dimensional governing equations for the stagnation point flow into a one-dimensional problem using a similarity transformation.[3] The transformed steady-state equations for species, energy, and stream function are discretized along the axial centerline using a finite difference method, with the resulting set of algebraic equations being solved using Newton's technique. Steady-state solutions are obtained through a robust dynamically adaptive multiple-weight arclength continuation algorithm, capable of passing around turning points.[40] For the low-pressure experiments considered below, a constant pressure reactor is simulated, i.e., only the surface species equations are solved.

The CHEMKIN formalism is used to calculate gaseous multicomponent transport properties, equilibrium constants of gas-phase reactions, and the thermodynamic properties of reacting mixtures.[18,19] For the homogeneous H_2 oxidation chemistry, the 20 reversible reactions/9 species reaction mechanism of Miller and Bowman[22,3] is used.

For "important" feature identification, sensitivity analysis is applied.[16,38] Within the context of this paper, important features include the slope of catalytic ignition temperature as a function of fuel composition and qualitative trends of the LIF OH signal intensities (e.g., the tail and maximum) as a function of temperature and fuel composition. In these cases, sensitivity

TABLE 2: Comparison of Model-Calculated Activation Energies with Various Experimental Data

	reaction	activation energy (kcal/mol) this work, $\theta^* = 1$	exptl value	references
(3f)	$H^* + O^* \rightarrow OH^* + *$	12.1	≤13	Anton and Cadogan[1]
			13.8	Eisert and Rosén[8]
			2.5	Williams et al.[41]
(3b)	$OH^* + * \rightarrow H^* + O^*$	24.4	≤29	Anton and Cadogan
			5	Williams et al.
(4f)	$H^* + OH^* \rightarrow H_2O^* + *$	12.4	16 ± 2	Anton and Cadogan
			16	Eisert and Rosén
			15	Williams et al.
(4b)	$H_2O^* + * \rightarrow H^* + OH^*$	18.4	25	Anton and Cadogan
			37	Williams et al.
(5f)	$2OH^* \rightarrow H_2O^* + O^*$	18.9	18 ± 3	Anton and Cadogan
			18	Eisert and Rosén
(5b)	$H_2O^* + O^* \rightarrow 2OH^*$	12.6	10	Anton and Cadogan
			31	Williams et al.

analysis is used to identify a reaction or a combination of reactions which have the largest impact on the feature of interest. Then, the pre-exponentials of the "important" reactions are refined through comparison of the model predictions to the experimental data (see below). Aside from the pre-exponentials, the expressions for the heats of chemisorption (discussed above) of surface species can also be refined by the same approach. An important advantage of our approach is that the number of surface species (i.e., the degrees of freedom in optimizing the heats of chemisorption) is typically much smaller than the number of surface reactions for these reaction systems. For the H_2/O_2 system, we prefer to estimate them from experiments rather than to optimize them (see adsorption−desorption steps).

Reaction Mechanism Performance

Below, we first compare energetics computed using the UBI-QEP framework with experimental data. Subsequently, reaction pre-exponentials are refined to derive a consistent reaction mechanism over a wide range of experimental conditions. Finally, model validation is carried out by comparing to an independent set of different experiments.

Comparison of Computed and Experimental Activation Energies. Computed activation energies using the UBI-QEP theory are compared in Table 2 (for surface coverage $\theta^* = 1$) to some experimental data reported in the literature. The comparison shows that the UBI-QEP computed values are in reasonable agreement with the experimental findings. For all reactions, the computed activation energies are within about 2 kcal/mol of the experimental data of Anton and Cadogan[1] and Eisert and Rosén,[8] with the exception of reaction 4b. Significant differences are seen when predicted values and the aforementioned experimentally determined parameters are compared to the parameters reported by Williams et al.[42] (e.g., see reaction 3f). While some of the differences can be attributed to shortcomings of the UBI-QEP theory or experimental errors, the assumptions involved in extracting activation energies from the actual data can have a more significant impact.[12] An additional factor for the differences between experiments may be due to different adsorbate surface coverages which are often unknown. For example, Anton and Cadogan report that their experiments have been performed for O* coverages less than 0.04. Williams et al., on the other hand, only report model calculated surface coverages based on their kinetic reaction mechanism for a limited number of cases.

As an illustration of the influence of surface adsorbate coverages on reaction energetics, the activation energies of all reactions at three limiting surface coverages are shown in Table 1. Our calculations indicate that, for some reactions, varying surface coverage can have a remarkable influence on the activation energies. For example, the formation of OH* via reaction 5b is predicted to exhibit an activation energy of 12.6 kcal/mol on a vacant surface and 34.1 kcal/mol at high O* coverages. This information provides interesting insight into the behavior of the catalyst surface under different reactor operation conditions (for possible windows of operation, see ref 27). For example, prior to reactor startup or catalytic ignition, H* is the dominant surface species, and so, we expect the activation energy for OH* formation via reaction 5b to be relatively high. Upon catalytic ignition, two different scenarios can occur.[27] Under fuel-lean conditions (the exact fuel-to-oxidant ratio is gas-phase transport dependent),[3] an excess of O_2 leads to a predominantly O* covered surface. On the other hand, for fuel-rich conditions, although H_2 is in excess, the low binding energy of H* will actually lead to relatively easy desorption of H* and the surface can be vacancy dominated. Such dramatic changes in reaction pathway energetics with different reactor operation conditions can be one explanation for the considerable discrepancy between experimentally estimated activation energies. For example, while the actual surface coverages are not known for the experiments of Williams et al.,[42] their computed surface coverages (based on their kinetic mechanism) indicate that, under some conditions, a high coverage of O* is seen (such as for inlet reactants of $H_2O + O_2$). Taking this into consideration, we see that our prediction of 34.1 kcal/mol for reaction 5b at high O* coverages is reasonable when compared with Williams et al.'s value of 31 kcal/mol.

One subtle point to mention is that the surface temperature can also influence the computed activation energies. This is because the computed activation energies depend on the gas-phase enthalpy of formation of the species involved in the reaction, which is temperature dependent. The values shown in Table 1 were computed for room temperature, and variances of up to ~1.5 kcal/mol are seen at 1200 K.

Refinement of Reaction Pre-exponentials. As discussed earlier, since the UBI-QEP theory only provides the energetics of surface reactions, we have relied on comparison with available experimental data from the literature to refine the pre-exponentials of reactions 1b, 4f, and 6b. Three different sets of polycrystalline platinum experimental data have been used, and the details of the experiments are discussed below.

The experimental results of the catalytic ignition temperature of 94% N_2 diluted H_2/O_2 mixtures as a function of composition are shown in Figure 1. The experimental data are from Rinemmo et al.[31] and Deutschmann et al.,[6] who used a polycrystalline platinum foil in a stagnation geometry. Figure 2 shows the LIF OH desorption data of Williams et al.,[42] for fixed reactant partial pressures of 0.3 Torr of O_2 and 0.2 Torr of H_2O. With O_2 and H_2O as reactants, OH* forms from H_2O^* dissociation and also from the recombination of the second H* of H_2O^* with O* resulting from O_2 dissociative adsorption. Finally, Figure 3 shows the experimental LIF OH signal as a function of H_2 composition at a fixed catalyst temperature of 1200 K. The experiments were performed by Wahnström et al.[41] under a total reactant pressure of 100 mTorr.

To refine the sticking coefficients and the pre-exponentials of the surface reactions, the sensitivity of the model predictions against "important" features from these three sets of experimental data have been analyzed. These "important" features include the catalytic ignition temperature and its variation with fuel composition (Figure 1), the maximum in the OH desorption rate (Figure 3), the tail of the OH desorption rate at high H_2/

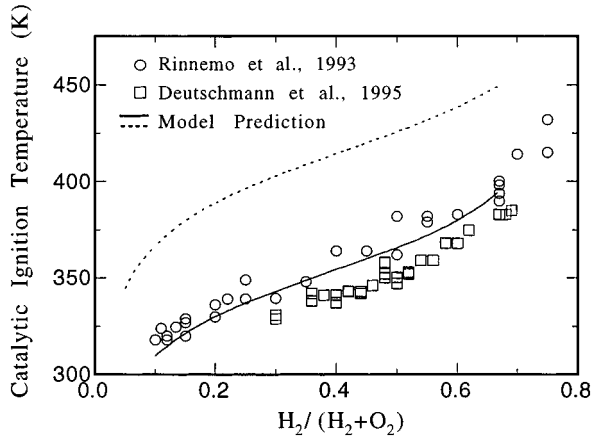

Figure 1. Comparison of model-predicted catalytic ignition temperature using various mechanisms ((solid line) this mechanism; (dash line) mechanism from ref 42) as a function of inlet composition with the experimental data of Rinemmo et al.[31] and Deutschmann et al.,[6] for reactor conditions of atmospheric pressure, 5 s^{-1} strain rate, and 94% N_2 dilution. Both the ignition temperature and the inhibition of ignition with increasing fuel composition are well captured by the model.

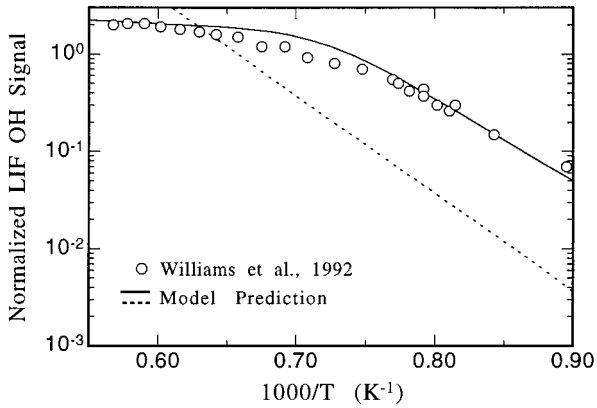

Figure 2. Comparison of model-predicted OH partial pressure just above the surface using various mechanisms ((solid line) this mechanism; (dash line) mechanism from ref 42) to the experimental LIF OH data of Williams et al.,[42] for a reactant pressure of 0.2 Torr of H_2O and 0.3 Torr of O_2. The model-predicted OH partial pressure has been normalized at one temperature to match the experimental data scale. The increased sensitivity in OH desorption with decreasing temperature is well captured by the model.

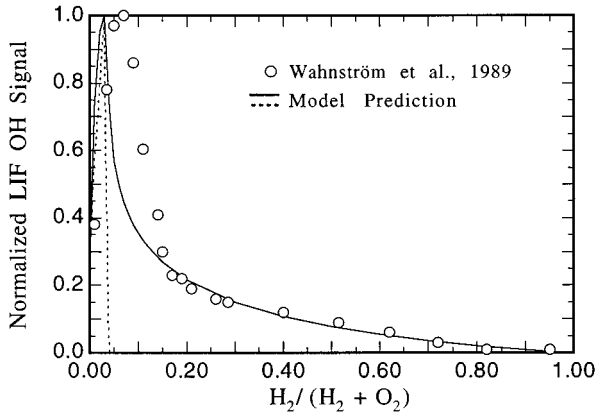

Figure 3. Comparison of model-predicted OH partial pressure just above the surface using various mechanisms ((solid line) this mechanism; (dash line) mechanism from ref 42) to the experimental LIF OH data of Wahnström et al.,[41] for a total reactant pressure of 100 mTorr and a surface temperature of 1200 K. The model-predicted OH partial pressure has been scaled by the maximum to match the experimental data. The maximum in LIF OH signal as well as the relative insensitivity at high H_2 compositions is well captured by the model.

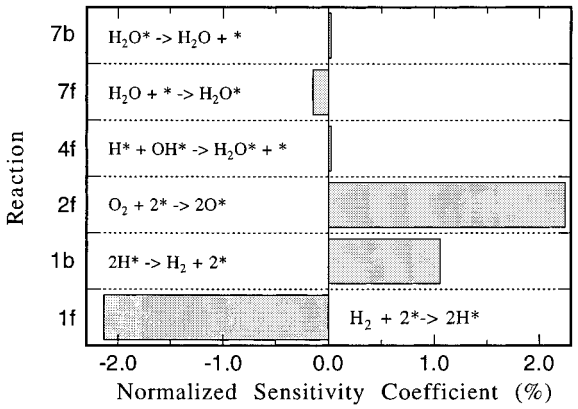

Figure 4. Sensitivity analysis of catalytic ignition to surface reaction pre-exponentials for reactor conditions of atmospheric pressure, 5 s^{-1} strain rate, and a reactant composition of 3% H_2, 3% O_2, and 94% N_2. The results indicate that only the adsorption of H_2 and O_2 and the desorption of H_2 are important for catalytic ignition temperature.

$(H_2 + O_2)$ ratios (Figure 3), and the decreased sensitivity in the OH desorption rate with increasing temperature (Figure 2). To analyze the sensitivity of these features to surface reaction parameters, sensitivity analyses have been performed. In particular, the response of the system to large and small perturbations in the sticking coefficients and the reaction pre-exponentials was studied numerically.

Figure 4 shows one such example (using the final reaction rate parameters listed in Table 1), depicting the influence of reaction pre-exponentials and sticking coefficients on catalytic ignition temperature for a 3.0% H_2 and 3.0% O_2 mixture in 94% N_2 dilution. For each reaction, the pre-exponential or the sticking coefficient was perturbed and the corresponding change in ignition temperature was recomputed. The normalized sensitivity coefficient, which represents the normalized change in ignition temperature with respect to the normalized size of the perturbation, is plotted for different reactions (for a rigorous sensitivity analysis method of bifurcation points based on linear algebra, see ref 16).

The sensitivity analysis results (Figure 4) on catalytic ignition indicate that only three reactions are important for catalytic ignition temperature, namely, reactions 1b, 1f, and 2f. Of these three reactions, both the sticking coefficients of H_2 and O_2 have already been fixed based on available literature data. So only the desorption pre-exponential of H* (1b) was optimized to 1.0×10^{12} s^{-1}. Similar analysis indicates that, for the maximum in OH desorption shown in Figure 3, the relative ratio of H_2 to O_2 sticking coefficients is important. For the LIF OH desorption tail at high $H_2/(H_2 + O_2)$ ratios (Figure 3) and the decreased sensitivity in LIF OH signal at high temperatures (Figure 2), both the desorption of OH* (6b) and the consumption of OH* via reaction 4f were found to be important. The optimized values of the pre-exponentials are summarized in Table 1, and the corresponding model predictions are shown as the solid line in Figures 1−3.

A point of caution is that although only the pre-exponentials of a handful of reactions have been optimized, this does not necessarily mean that the initially assigned values for the pre-exponentials of other reactions are accurate. A rigorous refinement of all the reaction pre-exponentials would require further comparisons with different types of experimental data and/or reaction systems for which these parameters become important. Furthermore, the optimized parameters also depend on the

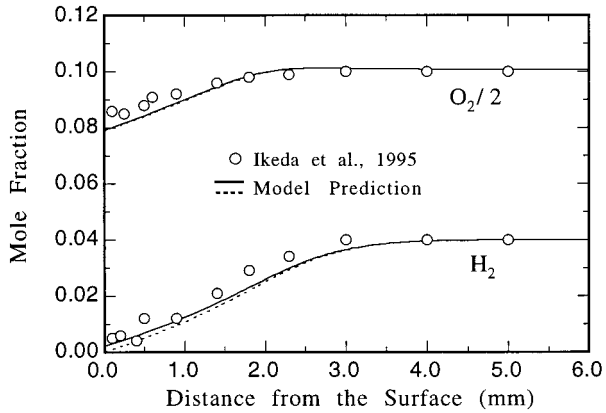

Figure 5. Comparison of model-predicted H_2 and O_2 mole fraction profiles using various mechanisms ((solid line) this mechanism; (dash line) mechanism from ref 42) along the length of a stagnation point flow reactor to the experimental data of Ikeda et al.,[15] for reactor conditions of atmospheric pressure, 31 s^{-1} strain rate, 773 K surface temperature, and 4% H_2 in air inlet composition. Both the species profiles and the boundary layer thickness are well predicted by the model.

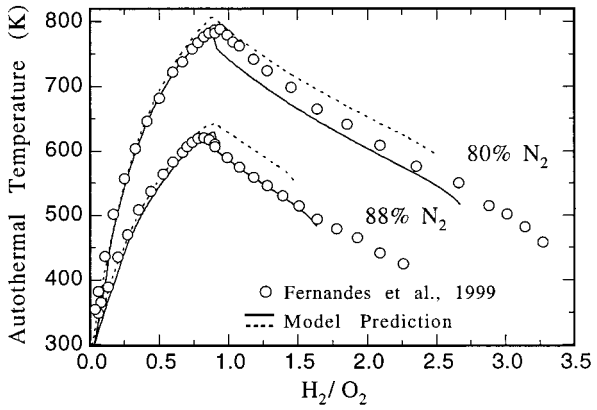

Figure 6. Comparison of model-predicted autotherms to the experimental data of Fernandes et al.,[9] for a stagnation reactor of atmospheric pressure, 5 s^{-1} strain rate, and two different N_2 dilutions of 88% and 80%. The catalytic autothermal temperatures are well captured by the model at both dilutions.

assumed functional forms and values of the heats of chemisorption (eqs 2−6).

The comparison between the experimental data and the refined surface reaction mechanism is quite reasonable. For the catalytic ignition (Figure 1), both the ignition temperature and the increase in catalytic ignition temperature with increasing H_2 composition is well captured by the simulations. While the fuel-rich catalytic ignition range is slightly underpredicted by the simulations when compared to the data of Rinnemo et al., it should be kept in mind that the model predicted ignitions are defined mathematically by a turning point (or the occurrence of hysteresis), and this condition can sometimes be hard to distinguish from the sudden onset of reactivity (without any hysteresis) in experiments. For the LIF OH desorption comparison shown in Figure 2, there is good agreement between the simulations and experimental results throughout the entire temperature range of ∼1100 to 1800 K. In particular, the increased sensitivity in OH desorption with decreasing temperature is well captured by the model. Finally, in Figure 3, both the maximum in LIF OH signal and the fuel-rich desorption tail are well predicted by the simulations. However, the model slightly underpredicts the location of the maximum. As mentioned above, analysis indicates that this maximum is sensitive to the sticking coefficients of H_2 and O_2. More specifically, decreasing the sticking coefficient of H_2 shifts the location of the maximum to higher $H_2/(H_2 + O_2)$ ratios, whereas the opposite trend holds for the O_2 sticking coefficient. Although the sticking coefficients of both H_2 and O_2 have been fixed by using reasonable experimental values, as mentioned above the sticking coefficient of H_2 increases with increasing surface roughness of platinum. On the basis of our analysis, we believe that the small difference in the location of the maximum seen in Figure 3 can be explained by assuming a more smooth surface (and hence a lower H_2 sticking coefficient) for Wahnström et al.'s system.

Model Validation. Since the experimental data presented in Figures 1−3 have been used to optimize the pre-exponentials of the surface reaction mechanism, it is important to perform additional comparisons without any parameter adjustments to evaluate the performance of the surface reaction mechanism. Figure 5 shows one such comparison against the experimental data of Ikeda et al.,[15] where the spatial profiles of H_2 and O_2 mole fraction are plotted along the length of a stagnation point flow reactor at a fixed catalyst temperature of 773 K and inlet conditions of 4% H_2 in air at 302 K. All the general features of the experimental results are well reproduced by the simulations, such as the length of the boundary layer (the spatial position at which H_2 and O_2 mole fractions deviate from inlet conditions) and the final conversion of H_2 and O_2 at the catalyst surface. This success is probably not very surprising, given the fact that, under these conditions, the system is mass transfer controlled.

One final comparison between the model and another set of experimental data is the catalytic autotherms of N_2-diluted H_2/O_2 mixtures of Fernandes et al.,[9] shown in Figure 6. Briefly, catalytic autothermal temperature is the catalyst temperature that corresponds to self-sustained combustion (desirable operation) of the fuel without any external heat provided to the system. In Figure 6, catalytic autothermal temperatures are shown as a function of H_2/O_2 ratios for two different dilutions of 80% and 88% N_2. Again, reasonable agreement is seen between the model predictions and the experimental data, with the model capturing both the range of catalytic autothermal temperatures as well as the maximum in the autothermal temperature. The model underprediction of the fuel-rich flammability limit at both dilutions is probably due to the high sensitivity of such points to heat losses and catalyst aging as discussed elsewhere.[9] However, despite these differences, the model performance is reasonable.

Comparison to Other Proposed Mechanisms. Despite the numerous experimental studies of H_2/O_2 chemistry on platinum, there is a limited number of surface reaction mechanisms.[7,9,30,42] All these mechanisms have been limited in scope by assembling most parameters from different experiments and refining the remaining ones by comparison to only one set of experimental data. Therefore, it is not surprising that, even for H_2 oxidation, predictions using these mechanisms are not always good. As an example, for all the experimental data considered, we have also plotted the model predictions using the H_2 surface mechanism of Williams et al.[42] (Figures 1−3, 5, and 6 in dashed lines). The comparison shows that the mechanism performs reasonably well for some cases, but poorly for the experimental LIF OH data. While the qualitative ignition trend with fuel composition is well captured (Figure 1), the ignition temperatures are overpredicted by ∼60 K. For the LIF OH data, only the maximum in OH desorption seen in Figure 3 is well represented, but slightly underpredicted. The species profiles (Figure 5) are well captured, mainly due to mass transfer

limitations. However, the fuel-rich flammability limit (Figure 6), where the desorption of H* becomes important, is underpredicted.

Conclusions

A new methodology has been presented for computing the parameters of metal-catalyzed surface reactions. This methodology combines the unity bond index−quadratic exponential potential theory of Shustorovich, reactor scale modeling, feature identification techniques for parameter refinement, and model validation. This approach has been applied to a model system, the platinum-catalyzed oxidation of H_2. Using available experimental data in the literature for adsorbate−adsorbate interactions, a surface reaction mechanism has been developed for H_2, which is thermodynamically consistent and takes into consideration the change in activation energies of reaction pathways with varying adsorbate coverages of surface species.

The model predictions have been compared against experimental data available in the literature to refine the preexponentials of some surface reactions. The resulting surface reaction mechanism successfully predicts a wide range of experimental data, such as LIF OH desorption as a function of both H_2 composition and temperature, catalytic ignition, catalytic autothermal temperatures, and species profiles. Extension to more complex fuels is straightforward and will be reported elsewhere.

Acknowledgment. Acknowledgment is made to the Office of Naval Research with Dr. G. D. Roy through a Young Investigator Award under Contract N00014-96-1-0786 and to the National Science Foundation (CAREER CTS-9702615) for support of this work. We thank Dr. D. Zerkle for his insightful comments on this work.

References and Notes

(1) Anton, A. B.; Cadogan, D. C. *J. Vac. Sci. Technol.* **1991**, *9*, 1890.
(2) Bui, P.-A.; Vlachos, D. G.; Westmoreland, P. R. *Ind. Eng. Chem. Res.* **1997**, *36*, 2558.
(3) Bui, P.-A.; Vlachos, D. G.; Westmoreland, P. R. Homogeneous Ignition of Hydrogen/Air Mixtures over Platinum. 26th Symposium (International) on Combustion, The Combustion Institute, Pittsburgh, 1996; p 1763.
(4) Campbell, C. T.; Ertl, G.; Kuipers, H.; Segner, J. *Surf. Sci.* **1981**, *107*, 220.
(5) Christmann, K.; Ertl, G.; Pignet, T. *Surf. Sci.* **1976**, *54*, 365.
(6) Deutschmann, O.; Schmidt, R.; Behrendt, F. Interaction of Transport and Chemical Kinetics in Catalytic Combustion of H_2/O_2 Mixtures on Pt.; 8th International Symposium on Transport Phenomena in Combustion, San Francisco, 1995; p 166.
(7) Deutschmann, O.; Schmidt, R.; Behrendt, F.; Warnatz, J. Numerical Modeling of Catalytic Ignition. 26th Symposium (International) on Combustion, The Combustion Institute, Pittsburgh, 1996; p 1747.
(8) Eisert, F.; Rosén, A. *Surf. Sci.* **1997**, *377*−*379*, 759.
(9) Fernandes, N. E.; Park, Y. K.; Vlachos, D. G. *Combust. Flame* **1999**, *118*, 164.
(10) Fisher, G. B.; Gland, J. L.; Schmieg, S. J. *J. Vac. Sci. Technol.* **1982**, *20*, 518.
(11) Frenklach, M.; Wang, H.; Goldenberg, M.; Smith, G. P.; Golden, D. M.; Bowman, C. T.; Hanson, R. K.; Gardiner, W. C.; Lissianski, V. *GRI-Mech- -An Optimized Detailed Chemical Reaction Mechanism for Methane Combustion*; Gas Research Institute, 1995.
(12) Fridell, E.; Elg, A.-P.; Rosén, A. *J. Chem. Phys.* **1995**, *102*, 5827.
(13) Fujimoto, G. T.; Selwyn, G. S.; Keiser, J. T.; Lin, M. C. *J. Phys. Chem.* **1983**, *87*, 1906.
(14) Gray, P.; Griffiths, J. F.; Scott, S. K. *Proc. R. Soc. London* **1984**, *A394*, 243.
(15) Ikeda, H.; Sato, J.; Williams, F. A. *Surf. Sci.* **1995**, *326*, 11.
(16) Kalamatianos, S.; Park, Y. K.; Vlachos, D. G. *Combust. Flame* **1998**, *112*, 45.
(17) Kalamatianos, S.; Vlachos, D. G. *Combust. Sci. Technol.* **1995**, *109*, 347.
(18) Kee, R. J.; Dixon-Lewis, G.; Warnatz, J.; Coltrin, M. E.; Miller, J. A. *A FORTRAN Computer Code Package for the Evaluation of Gas-Phase Multicomponent Transport Properties*; Sandia National Laboratories Report, SAND86-8246, 1990.
(19) Kee, R. J.; Rupley, F. M.; Miller, J. A. *The CHEMKIN Thermodynamic Data Base*; Sandia National Laboratories Report, SAND87-8215B, 1991.
(20) Ljungström, S.; Kasemo, B.; Rosén, A.; Wahnström, T.; Fridell, L. *Surf. Sci.* **1989**, *216*, 63.
(21) Luntz, A. C.; Harris, J. *Surf. Sci.* **1991**, *1991*, 397.
(22) Miller, J. A.; Bowman, C. T. *Prog. Energy Combust. Sci.* **1989**, *15*, 287.
(23) Mooney, C. E.; Anderson, L. C.; Lunsford, J. H. *J. Phys. Chem.* **1993**, *97*, 2505.
(24) Norton, P. R.; Davies, J. A.; Jackman, T. E. *Surf. Sci.* **1982**, *121*, 103.
(25) Norton, P. R.; Richards, P. J. *Surf. Sci.* **1974**, *44*, 129.
(26) Novakoski, L. V.; Hsu, D. S. Y. *J. Chem. Phys.* **1990**, *92*, 1999.
(27) Park, Y. K.; Bui, P.-A.; Vlachos, D. G. *AIChE J.* **1998**, *44*, 2035.
(28) Parker, D. H.; Bartram, M. E.; Koel, B. E. *Surf. Sci.* **1989**, *217*, 489.
(29) Pfefferle, W. C.; Pfefferle, L. D. *Prog. Energy Combust. Sci.* **1986**, *12*, 25.
(30) Rinnemo, M.; Deutschmann, O.; Behrendt, F.; Kasemo, B. *Combust. Flame* **1997**, *111*, 312.
(31) Rinnemo, M.; Fassihi, M.; Kasemo, B. *Chem. Phys. Lett.* **1993**, *211*, 60.
(32) Shustorovich, E. *Surf. Sci. Rep.* **1986**, *6*, 1.
(33) Shustorovich, E. *Adv. Catal.* **1990**, *37*, 101.
(34) Shustorovich, E.; Bell, A. T. *Surf. Sci.* **1991**, *248*, 359.
(35) Shustorovich, E.; Sellers, H. *Surf. Sci. Rep.* **1998**, *31*, 1.
(36) Somorjai, G. A. *Introduction to Surface Chemistry and Catalysis*; John Wiley & Sons, Inc.: New York, 1994.
(37) Thiel, P. A.; Madey, T. E. *Surf. Sci. Rep.* **1987**, *7*, 211.
(38) Tomlin, A. S.; Turanyi, T.; Pilling, M. J. *Elsevier Sci. J.* **1997**, *35*, 293.
(39) Verheij, L. K.; Hugenschmidt. M. B. *Surf. Sci.* **1998**, *416*, 37.
(40) Vlachos, D. G. *Chem. Eng. Sci.* **1996**, *51*, 3979.
(41) Wahnström, T.; Fridell, E.; Ljungström, S.; Hellsing, B.; Kasemo, B.; Rosén, A. *Surf. Sci. Lett.* **1989**, *223*, L905.
(42) Williams, W. R.; Marks, C. M.; Schmidt, L. D. *J. Phys. Chem.* **1992**, *96*, 5922.
(43) Zhdanov, V. P. *Surf. Sci.* **1986**, *169*, 1.